



KAPITEL 11 / CHAPTER 11 ¹¹
**IMPEDANCE METHOD FOR STUDYING THE ELECTRICAL
PROPERTIES OF LITHIUM-IRON SPINEL DOPED WITH RARE EARTH
METALS**

DOI: 10.30890/2709-2313.2024-32-00-026

Introduction

Nowadays, due to their dielectric and magnetic properties, spinel ferrites are widely used in radio engineering, radar, communication systems, and as memory carriers in computers. At the same time, the ability of such materials to the process of intercalation-deintercalation of lithium ions in their structure allows them to be considered as a promising material for the manufacture of the matrix of cathodes of portable lithium current sources [1].

The electrical properties of ferrites strongly depend on the method of synthesis, preparation conditions, chemical composition, cation distribution and microstructure of the material. The doping method is one of the most common in chemistry and technology as a way to control the structure of complex oxides and create new functional materials. The determining factor is the ability of the dopant ion to form an isomorphic substitution in the matrix structure of host [2].

The work [3] showed the prospects of replacing the traditional lithium-manganese spinel in lithium-ion batteries with a more stable lithium-iron oxospinel, more widely studied as a magnetic material. The similarity of the structures of lithium-manganese and lithium-iron spinel and the content of lithium ions in them were the reason for the attempt to use the latter polycrystalline system as a cathode material.

However, as shown in [1], its significant drawback is the low degree of electrochemical deintercalation of lithium from the $\text{Li}_{0.5}\text{Fe}_{2.5}\text{O}_4$ matrix due to the presence of Fe^{2+} ions in the structure, which restore part of the “guest” Li^+ ions to the atomic state and, thus, exclude the latter from an electrochemical process. Therefore, studies of the effect of modifying the electrophysical characteristics of lithium-iron spinel by isovalent replacement of iron ions with trivalent metal ions, including

¹¹*Authors: Vakalyuk Vasyl Mykhaylovych, Vakalyuk Andrii Vasylovych*



aluminum ions, have become relevant. Aluminum-doped lithium-iron spinels-ferrites with the general formula $\text{Li}_{0.5}\text{Fe}_{2.5-x}\text{Al}_x\text{O}_4$, synthesized by ceramic technology, have attracted the attention of researchers as stable ferrite materials widely used in modern technological systems [4,5].

The morphology, phase content, crystal structure of the spinel phase of the synthesized Al-substituted lithium-iron spinels depending on the composition and mode of heat treatment at the final stage of synthesis, and their electrophysical characteristics were investigated in works [6,7]. Research in [8] of the temperature dependence of the conductivity of the synthetic material showed that in the temperature range lower than 475K, the electronic component of the conductivity of these disordered systems dominates, which can be realized using two mechanisms: hopping and activation. It was shown in work [9] that in the region of temperatures higher than 475K in the synthesized $\text{Li}_{0.5}\text{Fe}_{2.5-x}\text{Al}_x\text{O}_4$ ceramics, the Li^+ -ion mechanism of conductivity becomes predominant. In this work the temperature-frequency dependences of Li^+ -ion conductivity at different values of the aluminum content were interpreted on the basis of a generalized phenomenological model of charge transfer in superionic conductors [10]. Thereat the values of the concentrations of conductivity Li^+ ions, their macroscopic and microscopic mobilities were obtained in the entire studied temperature range for different values of the aluminum content in the synthesized samples.

In recent years, in order to expand the range of electrophysical properties of lithium-iron spinels, which can be useful in various fields of technology, in addition to isovalent substitution of iron ions with aluminum ions, attempts are being made to substitute iron ions with ions of other elements. In this regard, the doping of lithium-iron spinels with ions of rare earth metals may be a promising direction. A number of works [11-13] have been published in scientific journals in which the structure, morphology and electromagnetic properties of several nanocrystalline iron spinels doped with rare earth metals using the «sol-gel» synthesis technology are investigated.

Atoms and ions of rare earth elements, with a constant valence of +3, have uncompensated spin moments in *f*-orbitals [14]. The ions of different rare earth



elements are quite close in their chemical properties, since their outer electron shells are identical - they all have the $5s^25p^6$ configuration. The radii of trivalent ions gradually decrease from 1,11 Å for cerium (Ce) to 0,94 Å for ytterbium (Yb) as we move from one element of the group to another. This phenomenon is called lanthanoid compression, thanks to which it is possible to control the properties of crystals containing rare earth elements to a large extent by selecting the required radius of the trivalent ion for the crystals.

Ions of rare earth elements have pronounced magnetic properties. The difference between the magnetic properties of the ions of the group of rare earth elements and the transition ($3d$) metals is that the spin moments of the $4f$ -electrons are «hidden» in the inner electron shell of the rare-earth element the radius of which is about 0,3 Å. In view of this, ferrites, synthesized on the basis of rare earth elements and widely used in technology, have a high electromagnetic Q factor. The reason for this is that the connection of the active «magnetic subsystem» that is excited in ferrites by an external electromagnetic field with thermal phonons is weak, that is, a kind of "shielding" of the magnetically active subsystem from thermal fluctuations occurs.

The temperature-dependent frequency dispersion of conductive and dielectric properties of lithium-iron spinels doped with two representatives of rare earth metals - lanthanum and yttrium, synthesized by the technology of «sol-gel» autocombustion has been studied in works [15,16].

11.1. Impedance method

The impedance method makes it possible to study the properties of physical and electro-chemical systems by observing the behavior of the system under the influence of external influences. It is based on the classical method of transfer functions modified according to the specifics of physical and electrochemical systems as research objects. The essence of this method is that the state of the system under study is disturbed by a sinusoidal signal and at the same time, the response signal caused by it at the output is



measured.

If the system is linear, then the output signal has the same frequency as the input, but differs in amplitude and phase. The relationship between signals on outputs and inputs determines the complex transfer coefficient of the system for the corresponding frequency. The dependence of this coefficient on the frequency forms the transfer function of the system.

Compared to other electrochemical methods, the impedance method provides the highest accuracy for a wide frequency range of the operating signal and provides detailed information both on the processes of electrochemical kinetics and on the properties of the surface and volume of the object under study.

Data analysis is based on the ability to represent the complex impedance as an equivalent circuit (structural models). The representation of the circle components is related to the parameters of the physical components in the materials.

Structural impedance models are flexible and operational working models that, in addition to full quantitative information about the behavior of the object under study in the frequency range, they must contain information about the physics of the processes taking place in this object. Therefore, such models are built from elements that, according to their physical content, correspond to the processes modeled with their help.

On the basis of Nyquist diagrams, which represent phase hodographs of the real and imaginary parts of the resistance of the system, it is possible to determine the important parameters of the system, which describe its conductive and dielectric characteristics and their frequency behavior in a wide frequency range. Measurements were carried out on an Autolab PGSTAT 12/FRA-2 impedance spectrometer in the frequency range of 0.01 Hz– 100 kHz.

Thus, the use of the main structural elements and the creation of equivalent circuits based on them allows to describe the behavior of the studied object in the frequency range with a high degree of reliability and to obtain information about the physics of the processes taking place in it.

Using an impedance spectrometer, the real and imaginary parts of the complex



impedance were obtained: $Z^* = Z' - jZ''$. Accordingly, the specific resistance of the material is $\rho^* = \rho' - j\rho''$, where $\rho' = Z'A/d$ and $\rho'' = Z''A/d$. A is a cross-sectional area and d is a thickness of the sample.

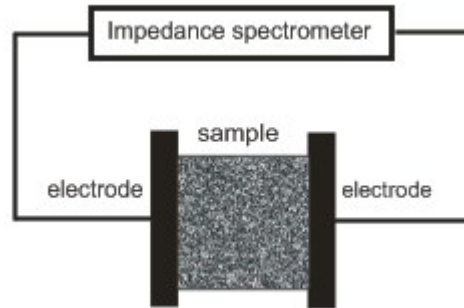


Figure 1 - Scheme of impedance measurement

Complex conductivity $\sigma^* = \frac{1}{\rho^*} = \sigma' + j\sigma''$, where $\sigma' = \rho'/M$ and $\sigma'' = \rho''/M$, with $M = |Z^*|^2 \left(\frac{A}{d}\right)^2$. It is assumed that the sample to which the alternating voltage U is applied is a capacitor, and current will flow through it $I = j\omega CU = j\omega(\varepsilon' - j\varepsilon'')C_0U = j(\varepsilon' - j\varepsilon'')A\varepsilon_0U/d$.

The current density in the material is equal to $i=I/A$ and the electric field intensity is $E=U/d$. Hence, $\sigma^* = \omega\varepsilon_0\varepsilon' + j\omega\varepsilon_0\varepsilon''$, or $\sigma^* = j\omega\varepsilon_0\varepsilon^*$. Then $\sigma' = \omega\varepsilon_0\varepsilon'' = \rho'/M$ and $\sigma'' = \omega\varepsilon_0\varepsilon' = \rho''/M$. The tangent of the dielectric loss angle is equal to $\tan \delta = \frac{\varepsilon''}{\varepsilon'}$.

11.2. Research methodology

The procedure of «sol-gel» autocombustion synthesis, which used for the synthesis of the samples, was as follows: for each composition, according to the formula, the necessary amounts of starting compounds were calculated, which were selected as crystal hydrates of iron nitrates $\text{Fe}(\text{NO}_3)_3 \cdot 9\text{H}_2\text{O}$, lithium LiNO_3 , lanthanum $\text{La}(\text{NO}_3)_3 \cdot 9\text{H}_2\text{O}$ and yttrium $\text{Y}(\text{NO}_3)_3 \cdot 9\text{H}_2\text{O}$. Citric acid acted as a chelating agent, and an aqueous ammonia solution was added to adjust the pH level of the reagent solution. Metal nitrates were dissolved in distilled water until complete dissolution with constant stirring with a magnetic mixer with the addition of citric acid. Ammonia solution (10%) was added dropwise to the precursors solution to adjust the required pH level (≈ 7). The



resulting solution was kept in a drying cabinet at a temperature of 343 K until the water was completely removed. After that, the dry gel was placed in an oven and heated to a temperature of 523-553 K at which the mixture ignited and the final product was formed. For conducting impedance studies, briquettes were created by pressing the obtained powder with the addition of a 10% solution of polyvinyl alcohol (PVA). The obtained samples with a diameter of 1 cm and a height of about 0.4 cm were subjected to sintering at a temperature of 873 K for 4 hours in an air atmosphere with slow cooling.

Conductive and dielectric characteristics of the synthesized compounds were calculated on the basis of experimental impedance spectra obtained on Autolab PGSTAT 12/FRA-2 spectrometer in the frequency range of 0.01 Hz - 100 kHz and the temperature range of 293-473 K. Temperature recordings were carried out with isothermal exposure every 20 K.

11.3. Study of temperature-frequency dependences of conductivity of lithium-iron spinel doped with rare earth metals.

The structure, morphology, phase composition, electrophysical properties of pure and aluminum-substituted lithium-iron spinels synthesized by the ceramic method have already been studied in detail in a number of research works [6-10]. Analysis of the temperature dependences of direct current conductivity in works [8,9] indicates the dominance of electronic conductivity in these ceramics in the temperature range of 295-475 K, and in the temperature range higher than 475 K, a cationic mechanism of conductivity appears and begins to dominate as the temperature increases, the activation energy of which lies within 0.9–1.4 eV.

Electronic conductivity can be realized using two mechanisms: hopping and activation [8]. Activation conduction is carried out by the drift in the electric field of free charge carriers generated in the conduction band either from the valence band or from the donor levels. The hopping mechanism of electrical conductivity in these



ceramics is mainly realized by the hopping of an electron between ions of the same element (in this case, these are ions Fe^{2+} and Fe^{3+}), which can be in more than one valence state, randomly distributed in crystallographically equivalent positions of the lattice [17]. In the temperature range of 295-350 K, the hopping mechanism dominates, the activation energy of which lies within the range of 0.10-0.14 eV, and in the range of 350-475 K, the activation mechanism dominates, the activation energy of which is approximately equal to 0.35 eV [8].

First, we will analyze the impedance temperature-frequency spectra of pure lithium-iron spinels synthesized by the technology of «sol-gel» autocombustion and compare them with the above mentioned results of the analysis of the impedance temperature-frequency spectra of these compounds synthesized by the ceramic method [18].

The impedance spectrum of pure lithium ferrite obtained by the "sol-gel" autocombustion technology in the entire investigated temperature range is presented in Figure 2. Taking into account the dimensions of the sample, the measured resistances were reduced to their specific values. A characteristic feature of Nyquist diagrams is that they are of the same type for all temperatures and consist of the arcs of two semicircles (truncated on the high and low frequency sides, as they are outside the working frequency range), describing the high-frequency and low-frequency regions of the spectrum. As the temperature increases, the radii of the high-frequency arcs of the hodographs decrease except for the last one, which corresponds to the temperature $T=473K$, which means that the resistance of the sample decreases as the temperature increases from 293K to 413K, and then begins to increase. In addition, it should be noted that the values of the resistances of the samples synthesized by the "sol-gel" autocombustion technology are 2-3 orders of magnitude lower than the values of the resistances of the samples synthesized by the ceramic method.

The impedance spectrum of this type can be modeled by an equivalent circuit consisting of an active resistance and two successive RC circuits (Figure 3).

According to the proposed model, the substance contains inclusions from grains and intergrain boundaries. The first component of the circuit corresponds to the ohmic

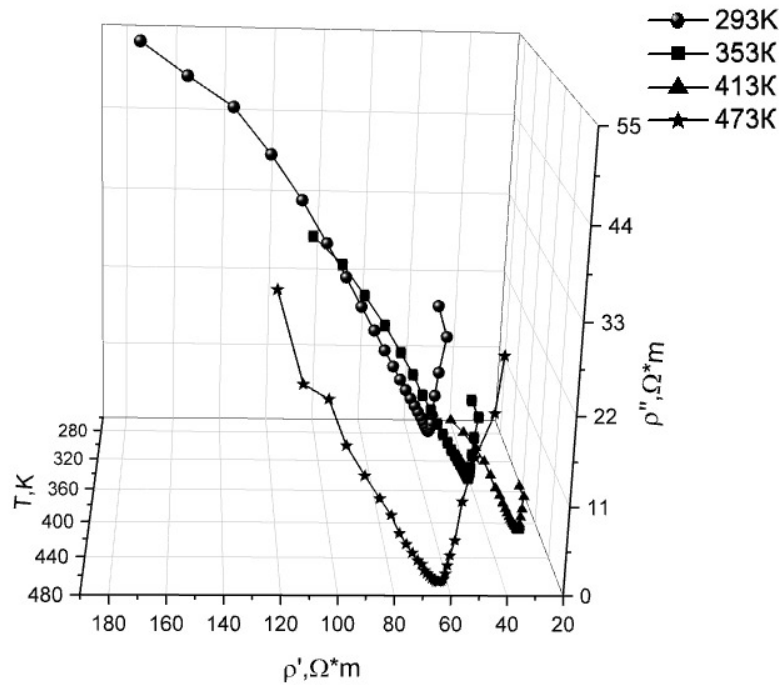


Figure 2 - Nyquist diagrams for $\text{Li}_{0,5}\text{Fe}_{2,5}\text{O}_4$ polycrystal at different temperatures

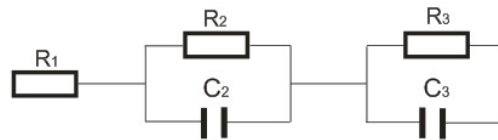


Figure 3- Equivalent circuit to the Nyquist diagram.

part of the resistance (R_1) of the sample which is independent of frequency. Objects modeled electrically as separate RC elements can be grains of the polycrystal (R_2C_2) and intergrain boundaries (R_3C_3).

Table 1 shows the values of specific conductivity σ_0 and dielectric permeability ϵ_0 at direct current for each component of the equivalent circuit.

Table 1

Component	Parameters	
	$\sigma_0, S \cdot m^{-1}$	ϵ_0
1	0,019	–
2	0,029	$2,59 \cdot 10^7$
3	0,012	$5,23 \cdot 10^8$

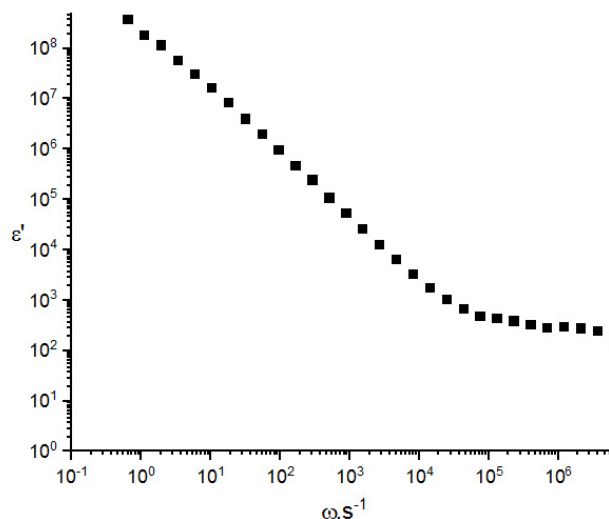


Figure 4 - Experimental dependence of the dielectric permeability of $Li_{0.5}Fe_{2.5}O_4$ spinel on the frequency at the temperature $T=293K$.

Dielectric permeabilities obtained directly from calculations using equivalent circuits agree quite well with direct measurements at low frequencies, as can be seen from Figure 4. The reason that the dielectric constant ϵ' of the studied samples increases strongly with decreasing frequency and reaches very large values, in our opinion, is the accumulation of electric charges transferred by Li^+ ions near the blocking electrodes and grain boundaries due to volume-charge (migratory) polarization, which can occur due to the presence of free crystallographic positions of spinels and the high mobility of lithium cations. The presence of a volume charge significantly increases the electrical capacity of the capacitor, and therefore the value of ϵ' .

To study the conductivity mechanisms of the synthesized samples of lithium-iron spinel, we will consider the frequency dispersion of the real part of the specific conductivity (σ') in the studied temperature range. Figure 5 presents the dependences of $\sigma'(\omega)$ obtained from Nyquist diagrams at different temperature values.

Analysis of the $\sigma'(\omega)$ curves presented in Figure 5 shows that:

1) at all temperatures of the studied range, in the region of low frequencies from $0.0628 s^{-1}$ to $10^2-10^3 s^{-1}$, the conductivity of spinel increases, and then in the interval $10^3-10^5 s^{-1}$ it almost does not change (increases very weakly) and, starting from the frequency $1.2 \cdot 10^5 s^{-1}$, decreases;

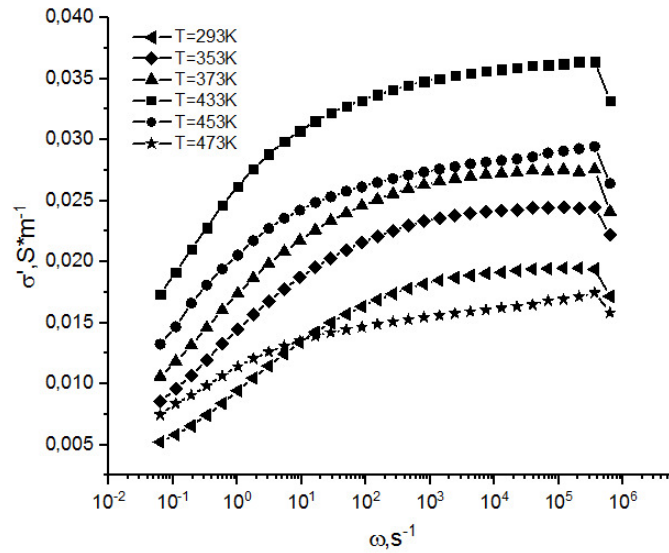


Figure 5 - Frequency dependences of the real part of the specific conductivity $\sigma'(\omega)$ of $\text{Li}_{0.5}\text{Fe}_{2.5}\text{O}_4$ spinel at different temperature values.

2) with an increase in temperature from 293K up to 433K, the conductivity of spinel at all frequencies increases, and then, after reaching a temperature of 433K, it drops sharply.

This behavior of conductivity depending on temperature and frequency may indicate the dominance in the synthesized sample of the electronic hopping mechanism of conductivity, which is realized through chain percolation processes $\text{Fe}^{+2} - e^- \leftrightarrow \text{Fe}^{+3}$ in octapositions of lithium oxoferrite spinel. At low frequencies, these processes are hindered by polarization processes caused by the displacement of lithium ions under the action of an electric field within single crystal grains. As the frequency increases, the influence of these processes decreases, and when it exceeds the frequency of natural vibrations of lithium ions, which is in the range of 10^2 - 10^3s^{-1} , the conductivity remains constant until reaching frequencies that exceed the frequency of natural vibrations of the valence electron in the ion Fe^{+2} ($\sim 10^5\text{c}^{-1}$). In this case, with increasing frequency, the time of electron movement in the direction of the field decreases and, therefore, an increasing number of such electrons do not reach the crystallographically equivalent positions of the lattice, where Fe^{+3} ions are located, so the conductivity decreases. Using Mott's theory, it is possible to calculate the



parameters characterizing the hopping mechanism of conductivity [15].

The value of the specific conductivity of the samples at direct current σ_0 at different temperatures was determined by the diagram $\sigma' - (\sigma'' - \varepsilon_0 \varepsilon_\infty \omega)$ ($\varepsilon_0 = 8,85 \cdot 10^{-12} \text{Ф/М}$, ε_∞ – the value of dielectric permeability at high frequencies, which was found from the Cole-Cole diagram $\varepsilon'' - \varepsilon'$). The dependence of σ_0 on temperature is presented in Figure 6.

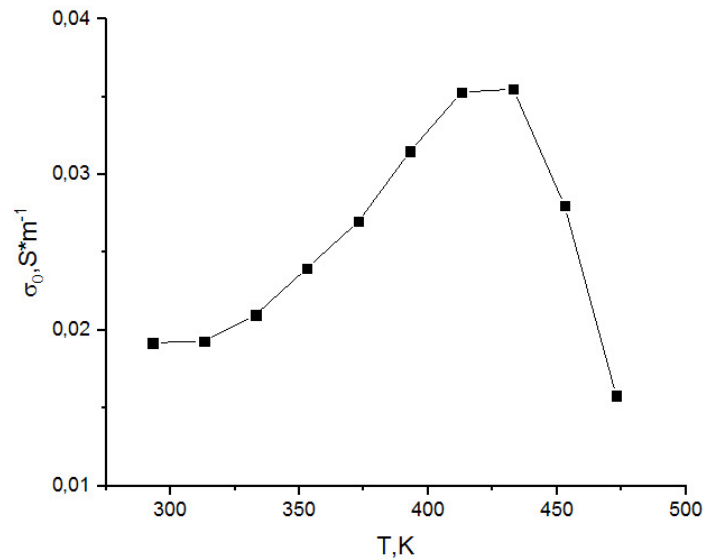


Figure 6 - Dependence of the direct current conductivity of $\text{Li}_{10.5}\text{Fe}_{2.5}\text{O}_4$ spinel on temperature.

The significant direct current conductivity of the obtained samples in comparison with the samples of pure and aluminum-substituted lithium-iron spinel obtained by the ceramic method [16] can be due to the fact that in them the single-crystal grains are quite closely adjacent to each other and the current flows along the surfaces of the contacting grains, which is evidenced by the photo of the microstructure of the sample, which is presented in Fig. 6a, and the high capacity of the grain boundary region ($C_3 \sim 10^{-4} \text{F}$).

A hopping mechanism of conductivity has an activation character because there is a local displacement of the electron cloud in the direction of the applied field and additional polarization occurs. The activation energy of this mechanism is low and, as shown in [8], does not exceed 0,15 eV for aluminum-substituted lithium-iron spinel ceramics.

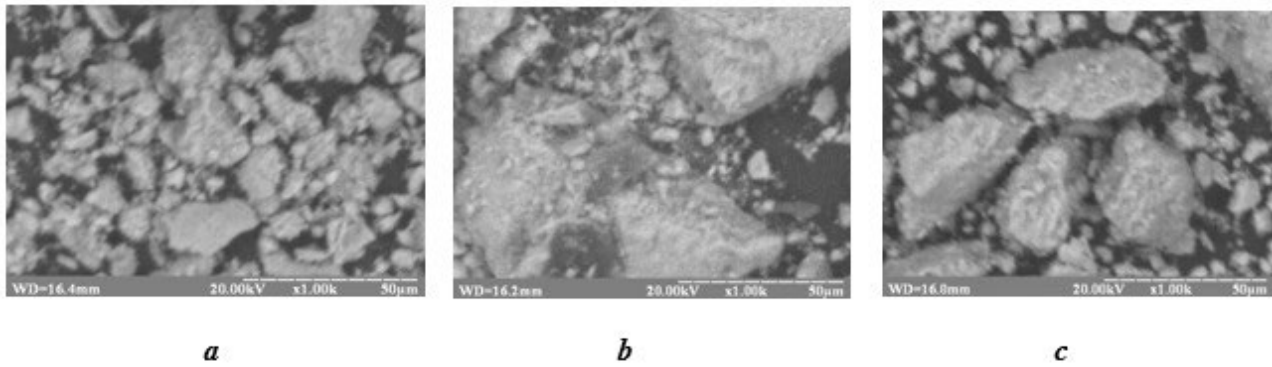


Figure 7 - SEM image of the structure: a – $\text{Li}_{0,5}\text{Fe}_{2,5}\text{O}_4$; b – $\text{Li}_{0,5}\text{Fe}_{2,5-x}\text{La}_x\text{O}_4$ ($x=0,03$); c – $\text{Li}_{0,5}\text{Fe}_{2,5-x}\text{Y}_x\text{O}_4$ ($x=0,03$).

The evidence of the realization of the activation mechanism of conductivity is the presence of a straight section on the Arrhenius curve (the temperature dependence of the specific conductivity of the direct current presented in the coordinates $\ln\sigma_0 \left(\frac{1}{T}\right)$). Activation conductivity is described by the equation:

$$\sigma = \sigma_{\infty} \cdot e^{-\frac{\Delta E}{2kT}},$$

where ΔE is the activation energy of the conduction process, k is the Boltzmann constant, and σ_{∞} is the value of the specific conductivity at $T \rightarrow \infty$. Then the activation energy is determined by the formula:

$$\Delta E = \frac{T_1 T_2 \ln \frac{\sigma_1}{\sigma_2}}{2k(T_1 - T_2)}$$

where temperatures T_1, T_2 and specific conductivities σ_1, σ_2 correspond to the coordinates of the edges of the rectilinear section on the Arrhenius curve.

On the Arrhenius curve for the sample of lithium-iron spinel synthesized by us using the "sol-gel" autocombustion technology, presented in Figure 8, two sections with different slopes of the approximating straight line can be distinguished. In the temperature interval of $293 \text{ K} \leq T \leq 313 \text{ K}$, which corresponds to the first section, with a slight slope of the approximating straight line, a hopping conduction mechanism is realized, the activation energy of which is equal to 0.04 eV.

As the temperature increases, the hopping mechanism breaks down and, starting at a temperature of 313 K, the activation mechanism becomes dominant up to a

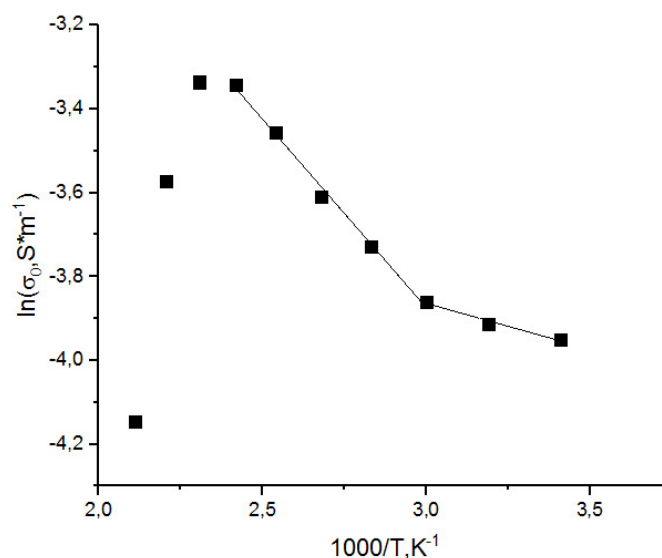


Figure 8 - Arrhenius curve for the sample of $\text{Li}_{0.5}\text{Fe}_{2.5}\text{O}_4$ spinel.

temperature of 433 K, when almost all valence electrons, leaving the Fe^{+2} ions under the influence of an external electric field, do not enter due to thermal vibrations of lattice nodes into Fe^{+3} ions, and become free, entering the internodal space (that is, from the donor levels of the band within which the hopping mechanism is realized, they pass into the conduction band). Thus, in the temperature range $313 \text{ K} \leq T \leq 433 \text{ K}$, which corresponds to the second section with a greater slope of the approximating straight line, an activation mechanism is realized, the activation energy of which is equal to 0.16 eV. As can be seen from figure 6, starting from a temperature of 433 K, there is a close to linear decrease in specific conductivity at direct current with increasing temperature, that is, due to the depletion of the donor band in which the valence electrons of Fe^{+2} ions are located, the metallic character of the conductivity is observed in the synthesized samples.

Let us now investigate how the replacement of iron ions with ions of two representatives of rare earth elements: lanthanum (La) and yttrium (Y) affects the electrical properties of lithium-iron oxospinel. Lanthanum and yttrium ions in chemical compounds can exist only in trivalent states. Most ions of the group of rare earth elements have pronounced magnetic properties due to the presence of electrons with unpaired spins in the 4f shell. They are paramagnetic. In lanthanum, with which



this group of elements begins, the $4f$ shell is empty and therefore the La^{+3} ion is diamagnetic. As a result of the replacement of iron ions Fe^{+2} and Fe^{+3} in lithium oxospinel (the magnetic moments of which are equal to $5,4\mu_B$ and $5,9\mu_B$, respectively) by ions of various lanthanides, which have different magnetic moments ranging from 0 in La^{+3} to $10,6\mu_B$ in Dy^{+3} , their magnetic properties will vary quite a lot. However, their electrical properties are similar, since all lanthanides have the same structure of outer electron shells and they differ only in ionic radii. Therefore, the results of the study of the influence of lanthanum doping of lithium-ferrite oxospinel on its electrical properties can be generalized to cases of doping with other lanthanides. Trivalent yttrium ions Y^{+3} , like lanthanum La^{+3} ions, are diamagnetic, but unlike them, they have a completely filled outer electron shell of $4s^24p^6$ and, therefore, a much smaller ionic radius.

Figure 9 presents experimental Nyquist diagrams for samples of $Li_{0,5}Fe_{2,5-x}La_xO_4$ composition with different lanthanum content.

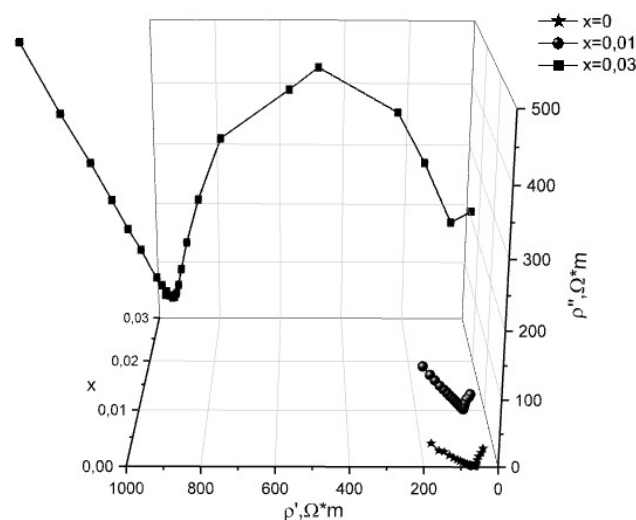


Figure 9 - Nyquist diagrams for the specific values of the complex impedance $\rho''(\rho')$ at the temperature $T=293K$ for the studied samples of the composition $Li_{0,5}Fe_{2,5-x}La_xO_4$ with $x=0;0,01;0,03$.

As can be seen from this figure, the specific complex resistance of the samples increases strongly with an increase in the content of lanthanum in them. Therefore, the direct current specific conductivity of the samples strongly decreases with increasing

lanthanum content. Table 2 shows the values of direct current conductivity and dielectric permeability of the components of the equivalent electrical circuit presented in Figure 2 for the $\text{Li}_{0,5}\text{Fe}_{2,5-x}\text{La}_x\text{O}_4$ sample with $x=0,03$.

Table 2

Component	Parameters	
	$\sigma_0, S \cdot m^{-1}$	ϵ_0
1	0,0023	—
2	0,0011	$1,58 \cdot 10^4$
3	0,0004	$7,50 \cdot 10^7$

The obtained values are consistent with the experimental frequency dependences of the real part of the dielectric permeability of $\text{Li}_{0,5}\text{Fe}_{2,5-x}\text{La}_x\text{O}_4$ for different values of the lanthanum content in the samples presented in Figure 10, from which it follows that as the lanthanum content in the samples increases, their dielectric permeability at low frequencies decreases.

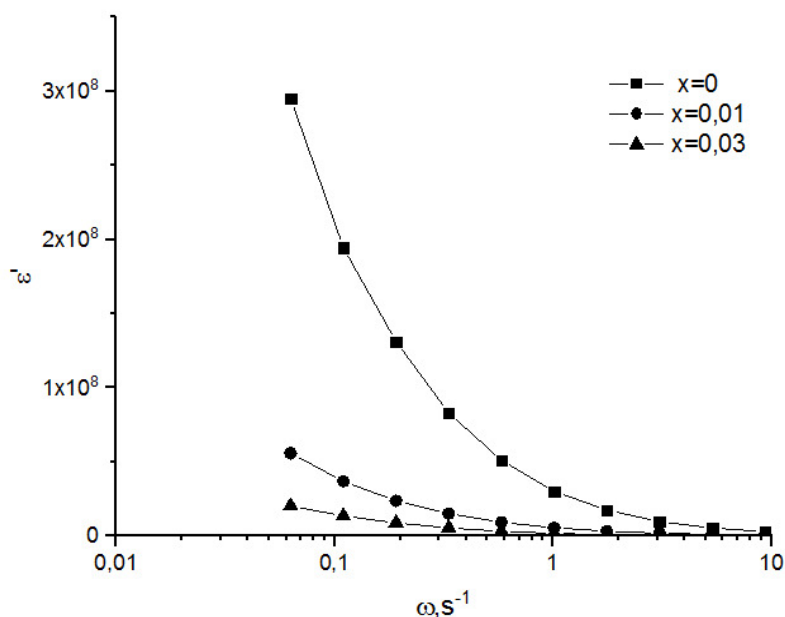


Figure 10 - Experimental dependences of the dielectric permeability of $\text{Li}_{0,5}\text{Fe}_{2,5-x}\text{La}_x\text{O}_4$ spinel on the frequency at the temperature $T=293\text{K}$ and different values of the lanthanum content in the samples ($x=0;0,01;0,03$).

Figure 7b shows a photograph of the microstructure of $\text{Li}_{0,5}\text{Fe}_{2,5-x}\text{La}_x\text{O}_4$ spinel for $x=0,03$. A comparative analysis of this photograph with the photograph of the



microstructure of pure lithium-iron spinel presented in Figure 7a shows that doping it with lanthanum leads to a violation of the homogeneity of the microstructure of the synthesized samples, i.e. to an increase in the dispersion of the sizes of single-crystal grains and an increase in the distance between them. Thereat as follows from the comparison of the data in Table 2 with the data in Table 1 and the analysis of the experimental curves $\varepsilon'(\omega)$ for different values of the lanthanum content presented in Figure 10, the specific conductivities and dielectric permeability at direct current, which correspond to the region of the grains and the region of intergrain boundaries decrease, and for the region of intergrain boundaries, they decrease significantly. These experimental facts lead us to the conclusion that the vast majority of La^{+3} ions are localized in the surface layer of single-crystal grains (since their radii are much larger than the radii of iron ions and they are not able to integrate into the middle of the crystal lattice of single-crystal grains), demolishing electronic conductivity in it, which is due to the hopping mechanism. As a result, the specific conductivity of grain boundary surfaces is significantly reduced, and therefore the total specific conductivity of the synthesized samples.

A decrease in the direct current conductivity of the synthesized samples with increasing lanthanum content is shown in Figure 11, which presents the experimental temperature dependence of σ_0 for different values of the lanthanum content.

On the experimental Arrhenius curves for samples of $Li_{0,5}Fe_{2,5-x}La_xO_4$ spinel with different lanthanum content, presented in Figure 12, one can distinguish rectilinear sections that are approximated by straight lines with different angles of inclination to the $1000/T$ axis, that may indicate the existence of two competing electronic conduction mechanisms: hopping and activation. The activation energies of these mechanisms can be determined by the tangents of these angles.

As follows from the results of the analysis of the inclination angles of the approximating straight lines presented in Figure 12, the presence of an impurity leads to an approximately a two-fold increase in the activation energy of both the hopping mechanism (from 0,04 eV to 0,08-0,1 eV) and the activation one (from 0,16 eV to 0,29-0,31 eV) compared to the case of pure (without impurities) lithium-iron spinel.

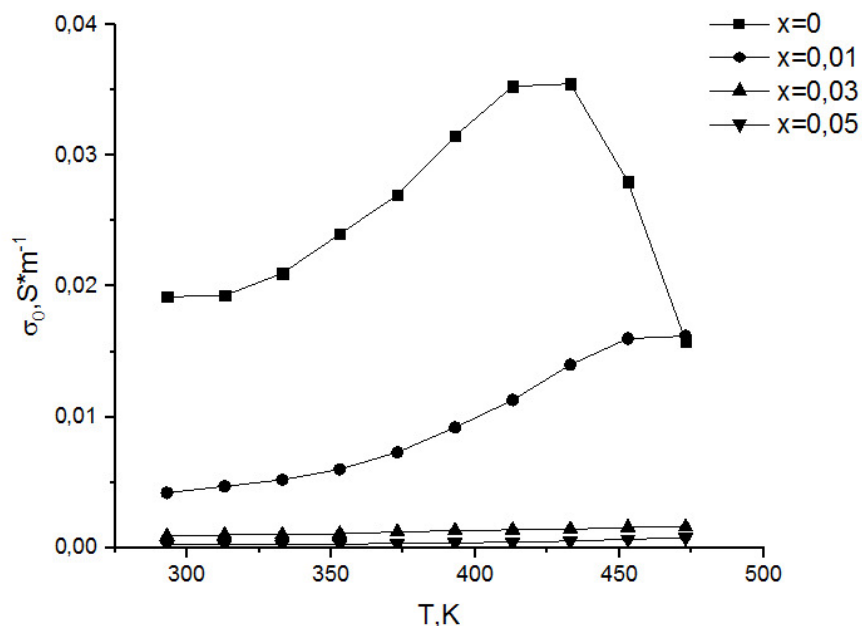


Figure 11 - Experimental temperature dependences of specific conductivity at direct current $\text{Li}_{0,5}\text{Fe}_{2,5-x}\text{La}_x\text{O}_4$ spinel for different values of lanthanum content in the samples ($x=0; 0,01; 0,03; 0,05$).

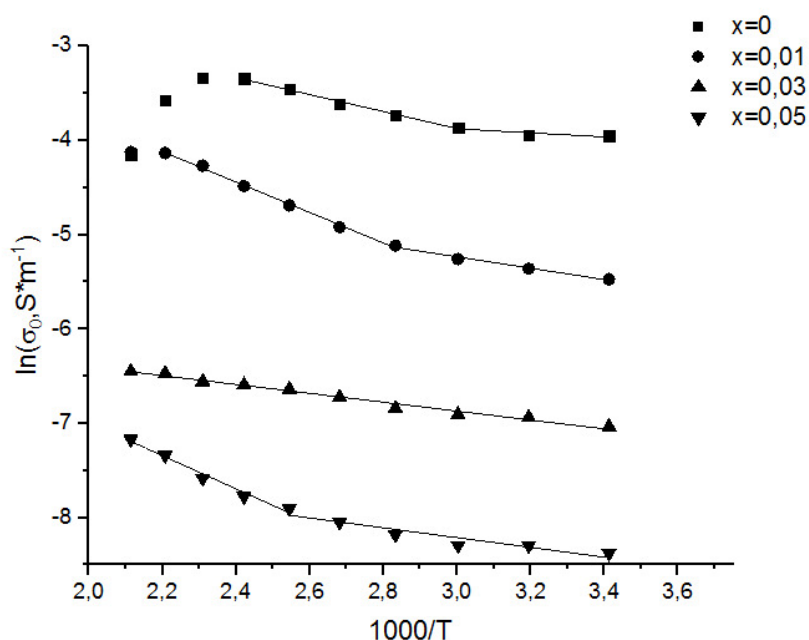


Figure 12 - Experimental Arrhenius curves with selected straight sections for $\text{Li}_{0,5}\text{Fe}_{2,5-x}\text{La}_x\text{O}_4$ spinel samples with different lanthanum content in the samples ($x=0; 0,01; 0,03; 0,05$).



Thereat with an increase in the impurity content, the temperature at which the hopping mechanism is replaced by the activation one increases. This change in conduction mechanisms can be visually interpreted using a simplified scheme of energy bands presented in Figure 13. According to this scheme, in the forbidden band, at the distance of the activation energy of the donor conduction mechanism from the bottom of the conduction band ΔE_a there is a narrow band 1, which is completely filled with valence electrons, which are located on Fe^{+2} ions. Above this band, at the distance of the activation energy of the hopping mechanism ΔE_h , there is a narrow empty band 2 in which the excited electrons do not linger and pass to the vacant energy levels of the original band 1. At low temperatures, the energy of the external electric field or thermal oscillations is sufficient only for the transition of electrons from band 1 to band 2. The number of electrons in band 1 is determined by the number of Fe^{+2} ions in the samples, which decreases as the number of La^{+3} impurity ions increases. The transition of electrons from band 1 to the conduction band determines the metallic character of conductivity, in which the mobility of electrons decreases with increasing temperature and the conductivity drops, which is exactly what is observed in Figure 11 for the case of a sample of pure lithium-iron spinel.

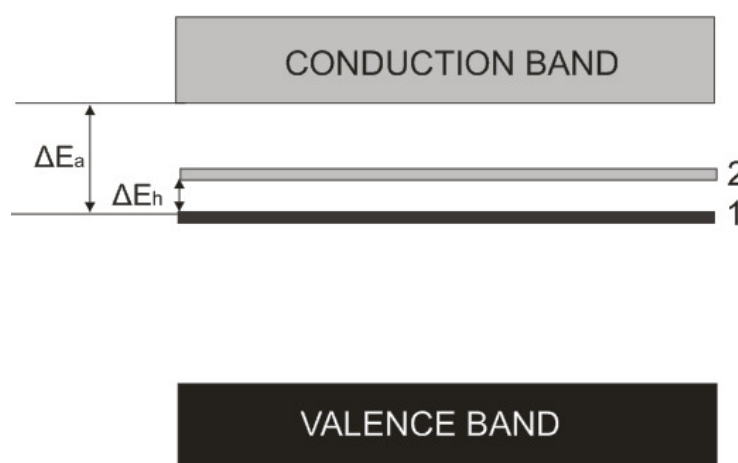


Figure 13 - Scheme of electronic energy bands of $Li_{0.5}Fe_{2.5-x}La_xO_4$ spinel.

As follows from Figure 14, in contrast to $Li_{0.5}Fe_{2.5}O_4$ spinel, the specific



conductivity of $\text{Li}_{0,5}\text{Fe}_{2,5-x}\text{La}_x\text{O}_4$ ($x=0,01$) spinel at all frequencies increases with increasing sample temperature, and in the frequency range $\omega > 10^5\text{s}^{-1}$ a maximum appears, which, in our opinion, can be associated with the appearance and growth of Li^+ -ion conductivity against the background of a sharp decrease in electronic conductivity due to the hopping mechanism. The Li^+ -ion mechanism of conductivity of lithium-iron spinel doped with aluminum was studied in detail by us on the basis of the generalized Jonscher model for superionic conductors [9].

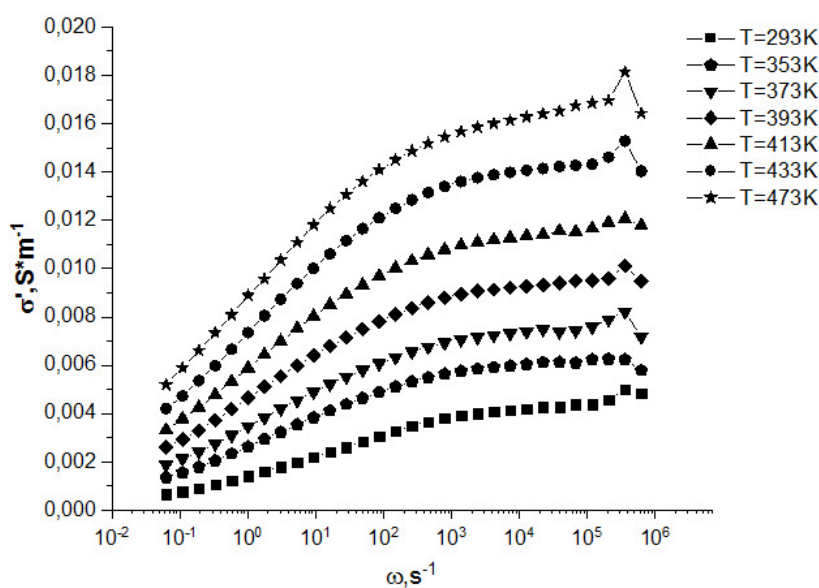


Figure 14 - Frequency dependences of the real part of the specific conductivity $\sigma'(\omega)$ of $\text{Li}_{0,5}\text{Fe}_{2,5-x}\text{La}_x\text{O}_4$ ($x=0,01$) spinel at different temperature values.

The effect of replacing iron ions with yttrium ions Y^{+3} on the electrical properties of lithium-iron spinels has the same character as the effect of lanthanum ions La^{+3} . Figure 7c shows a photograph of the microstructure of $\text{Li}_{0,5}\text{Fe}_{2,5-x}\text{Y}_x\text{O}_4$ spinel for $x=0,03$, from which it can be seen that the yttrium impurity, as well as the lanthanum impurity, leads to heterogeneity of the structure of the synthesized samples, which is characterized by a dispersion of grain sizes and an increase in the average distance between them.

The presence of an yttrium impurity in the synthesized samples reduces their conductivity significantly more than the presence of a lanthanum impurity.

The analysis of the experimental Arrhenius curves for $\text{Li}_{0,5}\text{Fe}_{2,5-x}\text{Y}_x\text{O}_4$ spinel



presented in Figure 15 shows that already with the content of yttrium impurity with $x=0.01$ in the entire studied temperature range only the activation donor conduction mechanism is possible. It is realized in the temperature range $293K \leq T \leq 413K$ with activation energy $\Delta E_a = 0,15 - 0,16$ eV. This means that yttrium ions due to their smaller radius are better embedded in the crystal lattice of the surface layer of lithium-iron spinel grains than lanthanum ions.

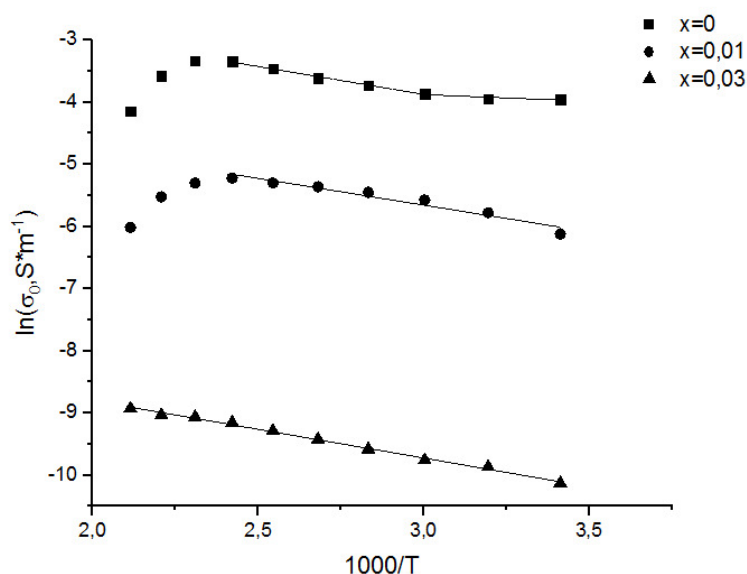


Figure 15 - Experimental Arrhenius curves with selected straight sections for $\text{Li}_{0,5}\text{Fe}_{2,5-x}\text{Y}_x\text{O}_4$ spinel samples with different yttrium content in the samples ($x=0$; 0.01; 0.03).

The temperature behavior of the frequency curves of conductivity for $\text{Li}_{0,5}\text{Fe}_{2,5-x}\text{Y}_x\text{O}_4$ spinel is similar to that for $\text{Li}_{0,5}\text{Fe}_{2,5-x}\text{La}_x\text{O}_4$ spinel. Figure 16 shows the temperature-frequency dependences of the conductivity of the $\text{Li}_{0,5}\text{Fe}_{2,5-x}\text{Y}_x\text{O}_4$ spinel sample with the yttrium content corresponding to $x=0,01$. From the analysis of these dependencies, it follows that:

1) in the temperature range $293K \leq T \leq 413K$ there is an increase, and in the range $413K \leq T \leq 473K$ there is a decrease in conductivity at all frequencies. The decrease in conductivity with increasing temperature can be explained according to the scheme of energy bands (Figure 13) by the depletion of the donor band due to the transition of



almost all electrons from it to the conduction band.

2) in the region of high frequencies $\omega \sim 10^5 \text{ Hz}$, the dependence of the conductivity on the frequency becomes non-monotonic, except for the curve that corresponds to the temperature $T = 293 \text{ K}$. This curve shows a monotonic decrease in conductivity in the frequency interval $10^4 \text{ Hz} \leq \omega \leq 10^5 \text{ Hz}$ and its growth in the frequency interval $10^5 \text{ Hz} \leq \omega \leq 10^6 \text{ Hz}$. This behavior may indicate the appearance and growth of Li^+ -ion conductivity against the background of a sharp decrease in electronic conductivity, as in the case of a lanthanum impurity.

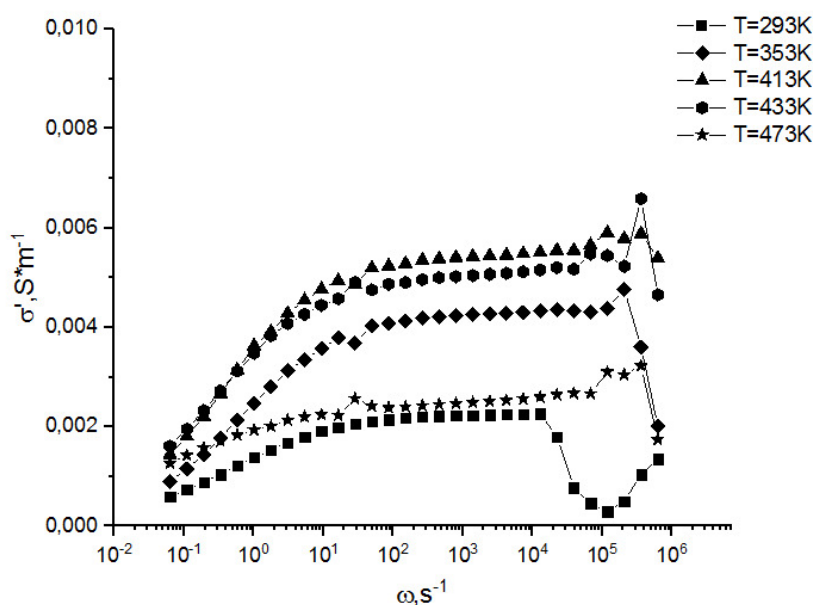


Figure 16 - Frequency dependences of the real part of the specific conductivity $\sigma'_1(\omega)$ of $\text{Li}_{0.5}\text{Fe}_{2.5-x}\text{Y}_x\text{O}_4$ ($x = 0,01$) spinel at different temperature values.

11.4. Study of frequency dispersion of complex permittivity of lithium-iron spinel doped with rare earth metals based on the generalized Jasher law.

Dielectric losses, which characterize the conversion of a part of electrical energy into thermal energy, are an important electrophysical parameter of the material. The magnitude of these losses, as well as their frequency dependence, is determined by the features of the polarization mechanism. Complex dielectric permittivity is a



particularly convenient parameter for describing the dependence of dielectric loss on frequency:

$$\varepsilon^*(\omega) = \varepsilon'(\omega) + i\varepsilon''(\omega) \quad (1)$$

The value of dielectric losses is mostly characterized by the tangent of the dielectric loss angle:

$$\tan \delta(\omega) = \frac{\varepsilon''(\omega)}{\varepsilon'(\omega)} \quad (2)$$

Dielectric losses usually change significantly when various impurities are introduced into the material. Depending on the concentration of impurities or structural defects, the value of dielectric losses can vary by tens or hundreds of times, while the change in the value of the real part of the complex permeability ε' can be relatively small. Therefore, dielectric losses are the most sensitive indicator of changes in the material structure. The study of dielectric losses and their dependence on impurities, structural defects, and other factors (temperature, intensity and frequency of the electric field, etc.) is of great interest for solid state physics.

We will investigate how the presence of rare earth metal impurities La and Y in small quantities affects the frequency dependence of the loss tangent, and therefore the structure of lithium-iron spinels.

The temperature-frequency dependences of the complex dielectric constant of the studied samples were calculated using experimental Nyquist diagrams. The frequency dispersion of the tangent of the dielectric loss angle $tg\delta$ in the synthesized samples of lithium-iron spinel without impurities for the range of investigated temperatures is shown in Figure 17.

In work [19], this behavior of the dispersion curves of the tangent of the dielectric loss angle with well-defined maxima is associated with the manifestation of the fractal structure of the material.

As can be seen from the figure, when the temperature increases, the local maximum of the dependence, which characterizes the resonant frequency of dielectric losses, shifts to the region of low frequencies. At the same time, the value of the maximum increases. Such a temperature dependence of the tangent of the dielectric loss angle is evidence that with increasing temperature, the electronic hopping mechanism is gradually destroyed and replaced by an activation one.

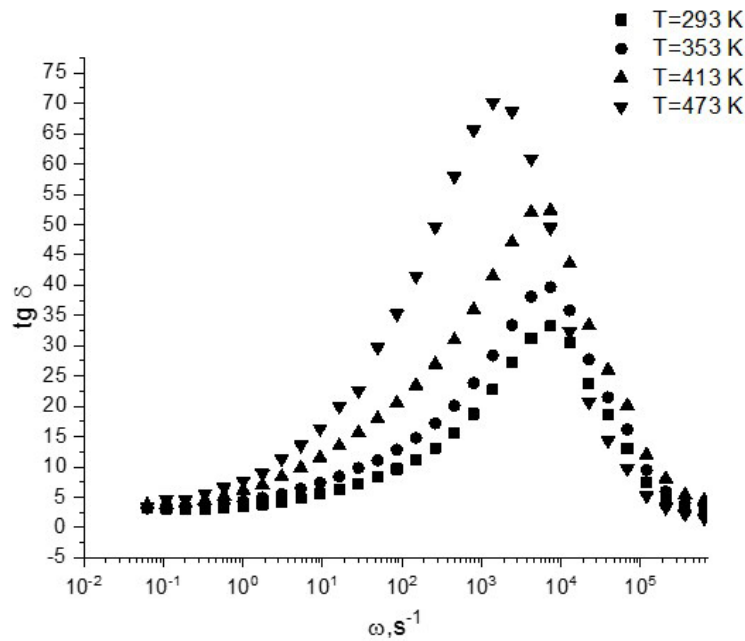


Figure 17- Experimental dependencies of the tangent of the dielectric loss angle on frequency for several temperature values in $Li_{0,5}Fe_{2,5}O_4$ spinel samples.

According to [19], in the generalized Jasher law, which satisfactorily describes the contribution of various mechanisms to the complex conductivity as a function of frequency for a wide class of different heterogeneous substances, regardless of their specific structure, except for the ordinary current caused by free current carriers $\vec{J}_0 = \sigma_0 \vec{E}$, and the polarization current $\vec{J}_p = \frac{\partial \vec{P}}{\partial t}$, caused by the emergence of electric polarization dipoles, we consider the current that is associated with the fractal structure $\vec{J}_{frac} = \sigma_{frac}(\omega) \vec{E}$ and is caused by local polarization with the resulting field of microstructural formations of the material. Then the total current is equal to:

$$\vec{J} = \vec{J}_0 + \vec{J}_p + \vec{J}_{frac} = \sigma(\omega) \vec{E}, \tag{3}$$

where the generalized conductivity normalized to the constant $\frac{\epsilon_0}{4\pi}$ ($\epsilon_0 = 8,85 \cdot 10^{-12} \frac{Ф}{М}$)

$$\sigma(\omega) = -i\omega(\epsilon(\omega) - \epsilon_\infty) \tag{4}$$

is expressed through the complex dielectric constant, which takes the form:

$$\epsilon(\omega) = \epsilon_\infty + \frac{\sigma_0}{i\omega} + \frac{\chi\tau^{-\nu}}{i\omega + (i\omega)^{1-\nu}\tau^{-\nu}} + R(i\omega). \tag{5}$$

The penultimate term of this expression reflects the contribution to the dielectric permittivity of the fractal structure, and the last term represents the contribution of

relaxation processes, which in the case of migration polarization is expressed by the Cole-Cole formula:

$$R(i\omega) = \frac{\varepsilon_0 - \varepsilon_\infty}{1 + (i\omega\tau)^\nu} \tag{6}$$

In formula (5), the value χ determines the dielectric susceptibility of the fractal structure.

Using simple algebraic transformations from formula (5), expressions for calculating the real and imaginary part of the complex dielectric constant can be found:

$$\varepsilon'(\omega) = Re[\varepsilon(\omega)] = \varepsilon_\infty + \frac{\chi\omega^{-\nu}\tau^{-2\nu} \sin\left(\frac{\nu\pi}{2}\right)}{\omega[1 + 2 \cos\left(\frac{\nu\pi}{2}\right)(\omega\tau)^{-\nu} + (\omega\tau)^{-2\nu}] + \frac{(\varepsilon_0 - \varepsilon_\infty)[1 + \cos\left(\frac{\nu\pi}{2}\right)(\omega\tau)^\nu]}{1 + 2 \cos\left(\frac{\nu\pi}{2}\right)(\omega\tau)^\nu + (\omega\tau)^{2\nu}} \tag{7}$$

$$\varepsilon''(\omega) = Im[\varepsilon(\omega)] = \frac{\sigma_0}{\omega} + \frac{\chi\tau^{-\nu}[1 + \cos\left(\frac{\nu\pi}{2}\right)(\omega\tau)^{-\nu}]}{\omega[1 + 2 \cos\left(\frac{\nu\pi}{2}\right)(\omega\tau)^{-\nu} + (\omega\tau)^{-2\nu}] + \frac{(\varepsilon_0 - \varepsilon_\infty)[1 + \sin\left(\frac{\nu\pi}{2}\right)(\omega\tau)^\nu]}{1 + 2 \cos\left(\frac{\nu\pi}{2}\right)(\omega\tau)^\nu + (\omega\tau)^{2\nu}} \tag{8}$$

Figure 18 shows the experimental frequency dependences of the tangent of the dielectric loss angle, together with their approximating theoretical curves according to formulas (2), (7) and (8) for four temperature values.

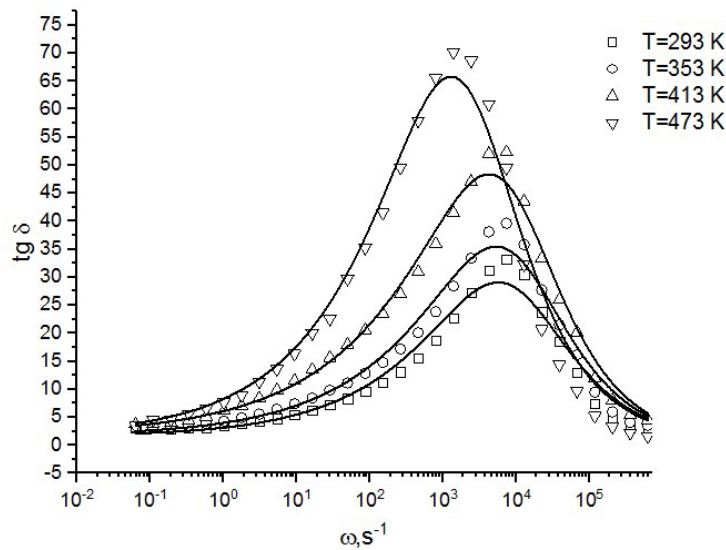


Figure 18 - Approximation of the experimental dependences of the tangent of the dielectric loss angle on the frequency for several temperatures by theoretical curves for a sample of $Li_{0.5}Fe_{2.5}O_4$ spinel free of impurities.

The frequency experimental dependences at these temperatures correspond to the values of the parameters of the approximating curves presented in Table 3.

Table 3

T, K	ϵ_{∞}	ϵ_0	σ_0, s^{-1}	ν	τ, s	χ
293	120	$3,0 \cdot 10^8$	$2,7 \cdot 10^{10}$	0,38	0,83	$3,91 \cdot 10^{12}$
353	113	$4,8 \cdot 10^8$	$3,4 \cdot 10^{10}$	0,36	2,0	$5,94 \cdot 10^{12}$
413	130	$7,9 \cdot 10^8$	$5,0 \cdot 10^{10}$	0,33	9,83	$9,79 \cdot 10^{12}$
473	180	$3,9 \cdot 10^8$	$2,3 \cdot 10^{10}$	0,38	30,8	$3,44 \cdot 10^{12}$

Let's investigate how the presence in $Li_{10.5}Fe_{2.5}O_4$ spinel of lanthanum impurity, which is the most common representative of rare earth metals, affects the dielectric losses and dielectric susceptibility of the fractal structure. Figure 19 shows the experimental frequency dependences of the tangent of the dielectric loss angle, together with their approximating theoretical curves obtained according to formulas (2), (7) and (8) for lanthanum-doped $Li_2Fe_{2.5-x}La_xO_4$ spinel at temperature of $T=293K$ for different impurity contents. The experimental frequency dependences at this temperature correspond to the values of the parameters of the approximating curves presented in Table 4.

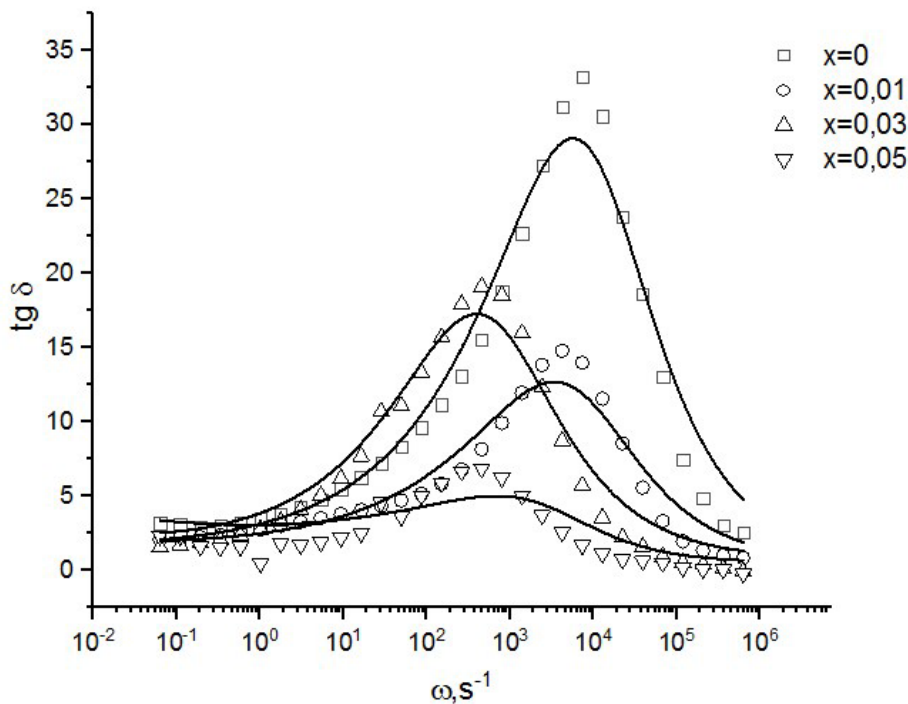


Figure 19 - Experimental dependencies of the tangent of the dielectric loss angle on the frequency at the temperature $T=293K$ and their approximating curves for samples of $Li_2Fe_{2.5-x}La_xO_4$ spinel with different values of x .



Table 4

x	ε_{∞}	ε_0	σ_0, s^{-1}	ν	τ, s	χ
0	120	$3,0 \cdot 10^8$	$2,7 \cdot 10^{10}$	0,38	0,83	$3,91 \cdot 10^{12}$
0,01	87	$5,6 \cdot 10^7$	$6,0 \cdot 10^9$	0,37	0,14	$2,8 \cdot 10^{11}$
0,03	98	$2,0 \cdot 10^7$	$1,2 \cdot 10^9$	0,42	1,84	$2,0 \cdot 10^{10}$
0,05	140	$1,0 \cdot 10^6$	$2,3 \cdot 10^{10}$	0,31	0,02	$1,5 \cdot 10^9$

As follows from Figure 19, as the content of lanthanum impurity in the samples increases, the value of the maximum of tangent of the dielectric loss angle decreases and it shifts to lower frequencies. Obtained theoretically, by approximating experimental frequency dependences with theoretical curves, the dielectric susceptibility χ of the fractal structure decreases significantly, by orders of magnitude.

There is a close correlation between the theoretical parameters ν , τ , χ , the fractal structure and the conductivity mechanism of the synthesized samples. By studying the effect on these parameters of the increase in the impurity content in the samples, we can predict how their fractal structure changes. The fact that the value of the exponent of the power of the frequency in the Jasher equation is within $0,31 \leq \nu \leq 0,42$ for all values of x indicates the realization of the hopping mechanism of conductivity in all samples at temperature $T=293K$. The hopping mechanism of electrical conductivity in these ceramics is mainly realized by the hopping of an electron between ions of the same element (in this case, these are ions Fe^{2+} and Fe^{3+}), which can be in more than one valence state, randomly distributed in crystallographically equivalent octohedral sites of the lattice [17].

The parameter τ means of the polarization relaxation time. As the temperature of the samples increases, it increases, which indicates a decrease in the mobility of electrons that participate in the hopping mechanism of conduction within the grains. Conversely, with an increase in the content of the lanthanum impurity in the samples, the relaxation time decreases, which is a consequence of the fact that the sizes of boundaries between grains increase. An exception to this rule for the

$Li_2Fe_{2,5-x}La_xO_4$ spinel sample with $x=0.03$ can be explained by the fact that groups of closely spaced grains formed in it due to the non-uniformity of the fractal structure.

The magnitude of the dielectric susceptibility χ of the fractal structure of the



sample is determined by the concentration of free charge carriers and their ability to move throughout the entire volume of the sample, which in turn depends on the features of the fractal structure (its homogeneity, grain sizes and grain boundaries). A sharp decrease, by orders of magnitude, in the dielectric susceptibility indicates that with an increase in the impurity content in the samples, the concentration of electrons participating in conductivity decreases, and the dispersion of grain sizes and the average distance between them increases. This is also evidenced by the decrease in the maximum value of the tangent of the dielectric loss angle and its shift to the low frequency region.

The effect of replacing iron ions with yttrium ions Y^{+3} on the electrical properties of lithium-iron spinels has the same character as the effect of replacing it with lanthanum ions La^{+3} . An impurity of yttrium, as well as an impurity of lanthanum, leads to heterogeneity of the structure of the synthesized samples, which is characterized by a dispersion of grain sizes and an increase in the average distance between them. However, the presence of an yttrium impurity in the synthesized samples reduces their conductivity much more strongly than the presence of a lanthanum impurity.

Figure 20 shows the experimental frequency dependences of the tangent of the dielectric loss angle, together with their approximating theoretical curves according to formulas (2), (7) and (8) for yttrium-doped lithium-iron spinel at a temperature of $T=293K$ with different impurity content. The experimental frequency dependences at this temperature correspond to the values of the parameters of the approximating curves given in Table 5.

As can be seen from Figure 20, the maxima of the approximating curves shift to lower frequencies with increasing yttrium impurity content in the samples, but unlike the case of doping spinel with lanthanum, their values decrease slightly. This means that both active and polarization components of the current through the samples decrease to the same extent. At the same time, there is a sharp decrease in the dielectric susceptibility χ and a sharp increase in the relaxation time already at $x=0.01$ and its invariance with a further increase in the content of the yttrium impurity.

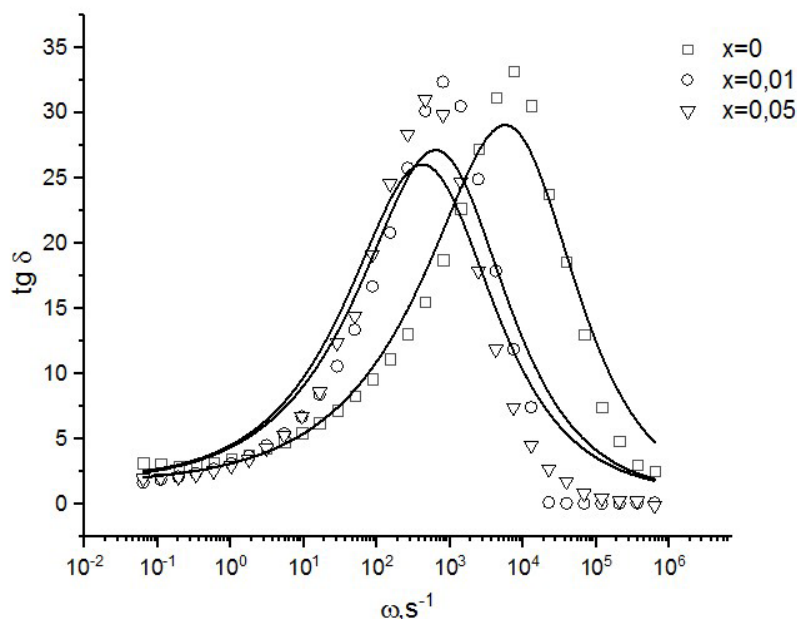


Figure 20 - Experimental dependencies of the tangent of the dielectric loss angle on the frequency at the temperature $T=293K$ and their approximating curves for samples of $Li_2Fe_{2.5-x}Y_xO_4$ spinel at different values of x .

Table 5

x	ϵ_∞	ϵ_0	σ_0, s^{-1}	ν	τ, s	χ
0	120	$3,0 \cdot 10^8$	$2,7 \cdot 10^{10}$	0,38	0,83	$3,91 \cdot 10^{12}$
0,01	167	$6,3 \cdot 10^7$	$3,1 \cdot 10^9$	0,42	3,8	$1,3 \cdot 10^{11}$
0,05	172	$3,0 \cdot 10^7$	$1,8 \cdot 10^9$	0,44	3,8	$3,5 \cdot 10^{10}$

Summary and conclusions

The conductivity of samples of lithium-iron spinel synthesized by the "sol-gel" autocombustion technology is significantly higher than the conductivity of samples synthesized by the traditional ceramic method. This is due to the fact that the microstructure of these samples in our case is more homogeneous and the current flows along the surfaces of the contacting single-crystal grains.

In the studied temperature interval of $293K \leq T \leq 473K$, two competing electronic mechanisms of conductivity can be realized: hopping and activation. The hopping mechanism dominates in the region of low temperatures and corresponds to the transition of electrons under the influence of an external electric field from the donor



band 1 to the empty band 2 which are located in the band gap (according to the scheme of energy bands). In the region of higher temperatures, the hopping mechanism changes to an activation one, which corresponds to the transition of electrons under the influence of temperature from the donor band to the conduction band. With a further increase in temperature, the donor band is emptied and all electrons from it pass to the conduction band. Then the metallic character of conductivity is realized.

Doping lithium-iron spinel with ions of rare earth metals leads to a sharp decrease in its conductivity. The first reason for this is a violation of the homogeneity of the microstructure of the synthesized samples (an increase in the size dispersion of single-crystal grains and an increase in the distances between them), and the second one is the destruction of the hopping mechanism of conductivity (a decrease in the concentration of Fe^{+2} ions by replacing them with trivalent ions of rare earth metals, and as well as the resulting increase in the average distance between iron ions in the crystal lattice of the grain) In the case of doping lithium-iron spinel with yttrium ions, against the background of a sharp decrease in electronic conductivity in the high-frequency region of the spectrum, Li^+ ion conductivity may appear even at low temperatures.

The generalized Jasher's law, which we applied to the study of polarization processes, quite correctly describes the experimental temperature-frequency dependences of the tangent of the dielectric loss angle of lithium-iron spinel synthesized by the «sol-gel» autocombustion technology and doped with rare earth metal impurities. On its basis, it is possible to analyze the evolution of the fractal structure with a change in the temperature of the studied samples and the concentration of the impurity, estimate the average size of its grains, obtain a value of its dielectric susceptibility, and also draw a conclusion about the dominant conduction mechanism in the given temperature range.

It has been determined that an increase in the content of lanthanum and yttrium impurities in the samples leads to an increase in the inhomogeneity of the fractal structure (an increase in the dispersion of the sizes of single-crystal grains and intergrain boundaries) and the destruction of the electronic hopping conduction mechanism. Moreover, in the presence of yttrium impurity, this destruction is stronger



than in the presence of lanthanum. This is most likely due to the fact that the radius of the yttrium ion is smaller than the radius of the lanthanum ion and it more easily replaces iron ions in the crystal lattice of the surface layers of monocrystalline grains of lithium-iron spinel.